

Feedback-controlled ion beam sculpting apparatus

Derek M. Stein

Harvard University, Division of Engineering and Applied Sciences, 17 Oxford Street, Cambridge, Massachusetts 02143 and Department of Nanoscience, Delft University of Technology, Lorentzweg 1, 2628 CJ, Delft, The Netherlands

Ciaran J. McMullan

Harvard University, Department of Physics and Division of Engineering and Applied Sciences, 17 Oxford Street, Cambridge, Massachusetts 02138

Jiali Li

Harvard University, Department of Physics and Division of Engineering and Applied Sciences, 17 Oxford Street, Cambridge, Massachusetts 02138 and Department of Physics, University of Arkansas, Fayetteville, Arkansas 72701

Jene A. Golovchenko

Harvard University, Department of Physics and Division of Engineering and Applied Sciences, 17 Oxford Street, Cambridge, Massachusetts 02138

(Received 22 October 2003; accepted 4 December 2003; published 11 March 2004)

We report the design of an “ion sculpting” instrument that enables the controlled fabrication of nanometer-sized structures in solid-state materials. The instrument employs a beam of kilo-electron-volt argon ions that impinge on a solid-state membrane containing prefabricated structures such as holes, slits, or cavities whose properties are to be modified. By controlling both the ion beam parameters and sample temperature, the instrument can be adjusted to either deliver or remove material from these articulations, for example opening or closing holes of various shapes. The instrument is unique in its use of feedback control for the crafting of structures that define a hole through which a component of the incident ion beam is permitted to pass and be monitored. Electrostatic ion optics refocus ions transmitted unimpeded through the hole, onto a detector capable of registering single ions. The transmission rate is a direct, real-time measure of the transmitting area that is used as a feedback signal to trigger the termination of the ion irradiation process precisely when a desired dimension is obtained. The ions thus serve the dual role of modifying and measuring the size of the nanoscale structures. The sensitivity of the ion beam sculpting apparatus to atomic-scale material rearrangement at the perimeter of a hole also enables the study of ion beam induced material transport at solid-state surfaces. The utility of the instrument as a fabrication tool has been demonstrated by the fabrication of nanopores used for recent single-molecule biophysics studies. © 2004 American Institute of Physics. [DOI: 10.1063/1.1666986]

I. INTRODUCTION

We required isolated single-nanometer-scale holes, or “nanopores,” in thin insulating solid-state membranes for use at the heart of a device capable of detecting and manipulating individual DNA molecules. This need presented a significant technological challenge since the minimal feature size accessible by standard fabrication techniques is typically limited to tens of nanometers, as in the case of electron beam lithography. The fabrication of \sim nanometer scale holes in synthetic polymer films has been reported using a high-energy ion track etch technique,¹ however the ultra-high aspect ratio structures do not offer the necessary spatial resolution nor the compatibility with semiconductor processing techniques that we sought. The only established technique for fabricating suitable holes \sim 10 nm in diameter was developed by Ralls *et al.*,² who used electron beam lithography to expose a small spot on a free-standing membrane of silicon nitride. A reactive ion etch process that etched through the membrane was timed to stop shortly after the formation of a

hole. This method is limited, however, by the fact that it is “open-loop” because there is no way of directly knowing when it would be optimal to stop the process—a limitation that is common to all standard open-loop fabrication techniques.

A nanofabrication technique that we call “ion beam sculpting” was developed to circumvent the limitations of an open-loop etch. The ion beam sculpting apparatus (Fig. 1) incorporates feedback into the fabrication process to gain dimensional control over synthesized holes at the single nanometer length scale: In the instrument, a freestanding membrane surface containing an initial \sim 100 nm hole or bowl-shaped cavity is exposed to a normal beam of low energy ions. From simple geometrical considerations, the area of the hole is equal to the argon transmission rate divided by the incident flux. The rate of argon transmission through the hole is therefore a direct measure of its size, and is detected to provide the feedback signal necessary to trigger the extinction of the ion beam when the desired hole size is obtained. By controlling important experimental parameters such as

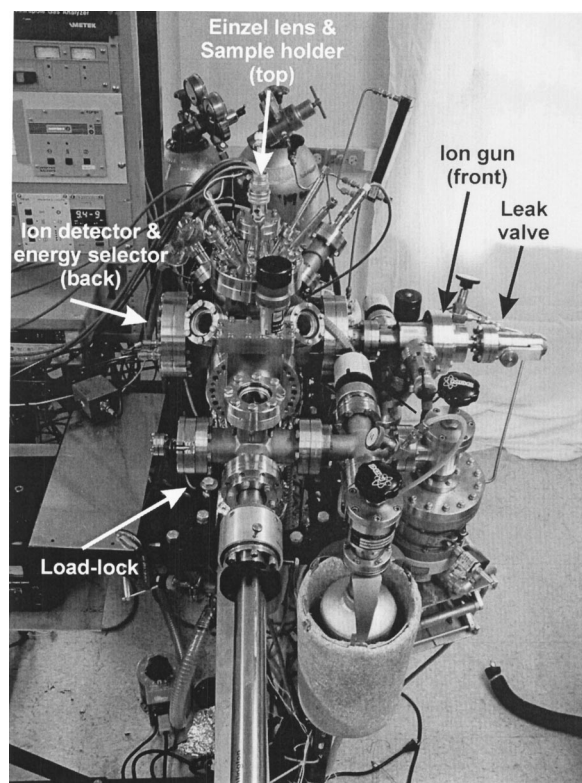


FIG. 1. The feedback-controlled ion beam sculpting apparatus.

sample material, temperature, ion flux, and ion beam time structure, it was discovered that the hole can be made to either open *or* close.³ For this reason we refer to the process as ion beam “sculpting” rather than simply “etching” or “sputtering.”

II. INSTRUMENT DESIGN

A schematic of the feedback-controlled ion beam sculpting apparatus shown in Fig. 2 illustrates the main components of the apparatus and the feedback loop that controls the ion beam. A differentially pumped ion gun (VG Microtech, East Grinstead, UK, Model EX05) bombards the surface of a sample with an argon ion beam of energy 0.5 to 5 keV. An electron gun (Kimball Physics, Wilton, NH, Model FRA-2X1-1) floods insulating surfaces with 50 eV electrons during ion beam exposure to neutralize surface charging effects.

The system is housed in a vacuum chamber pumped to 10^{-9} mbar by a turbomolecular pump (Pfeiffer TMU 260). A typical 3 keV argon ion beam is focused to a spot size of ~ 0.4 mm, with a typical (but adjustable) beam current of $0.2 \mu\text{A}$. This corresponds to approximately 10^{12} ions incident on the sample per second, and an ionic flux of $10^{15} \text{Ar}^+ \text{cm}^{-2} \text{s}^{-1}$. A nanopore with a diameter of 1 nm is therefore expected to transmit $\pi \times \text{radius}^2 \times \text{flux} = \sim 8$ argon ions per second. This expected transmission rate highlights two important requirements for the ion sculpting apparatus: First, every transmitted ion represents information crucial to the fabrication process that cannot be discarded. Second, considerable shielding is necessary to prevent any of the $\sim 10^{12}$ incident ions from masking the signal of interest, which is smaller by roughly 11 orders of magnitude.

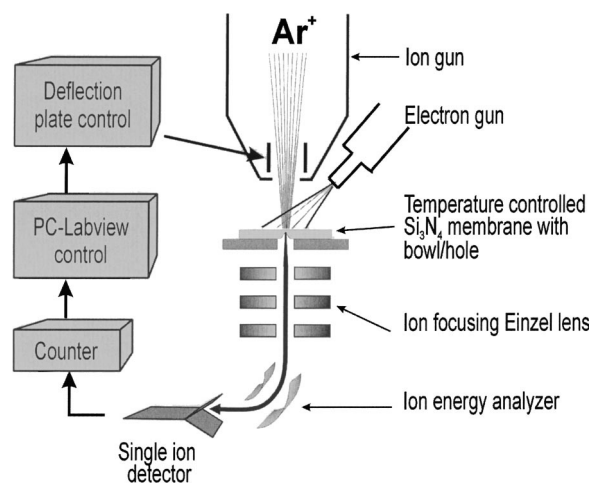


FIG. 2. Schematic of the feedback-controlled ion beam sculpting tool. The detection of ions transmitted through the sample membrane provides the physical signal necessary for the feedback loop to control the incident ion beam.

An electrostatic Einzel^{4–6} lens positioned directly behind the sample refocuses the transmitted ion beam. In order to unambiguously detect only the ions transmitted unimpeded through the nanopore, the focused, transmitted ion beam is deflected through 60° by an electrostatic, energy-selective deflection system onto an electron multiplier-style Channeltron (Burle Electronics, Lancaster, PA) single-ion detector. The electrical pulses arising from the detection of individual ions are first conditioned by a preamplifier, and then counted by a digital pulse counter (HP 53131A, Palo Alto, CA). The counting rate is monitored by a computer, and compared to an adjustable threshold value. When the counting rate crosses the threshold, a signal is sent to a power supply that applies 200 V across the deflection plates of the ion gun, thereby deflecting the beam ~ 5 mm off the sample and halting the ion beam sculpting process. The ion beam can also be extinguished based on a more complex analysis and extrapolation of the transmitted ion data.

III. ION OPTICS

The task of the ion optics system is to direct every ion transmitted through the hole in a sample onto the detector while excluding signals from scattered particles, optical emissions, and secondary charged particles. All electrostatic focusing and deflection elements were machined out of stainless steel, and their design was aided by ion trajectory simulations performed by the computer program, SIMION (<http://www.srv.net/~klack/simion.html>). A cross-sectional diagram of the ion optics is shown in Fig. 3. A modular system design was implemented for ease of maintenance and modification, with the sample holder and electrostatic focusing system mounted on one flange, and the detector and 60° deflection system mounted on another. All electrical feedthroughs needed for each electrostatic element were located on its respective flange.

The ion gun, mounted on the “front” flange of the chamber, delivers a beam of 3 keV argon ions to a sample surface in the normal direction. The beam is focused on a freestand-

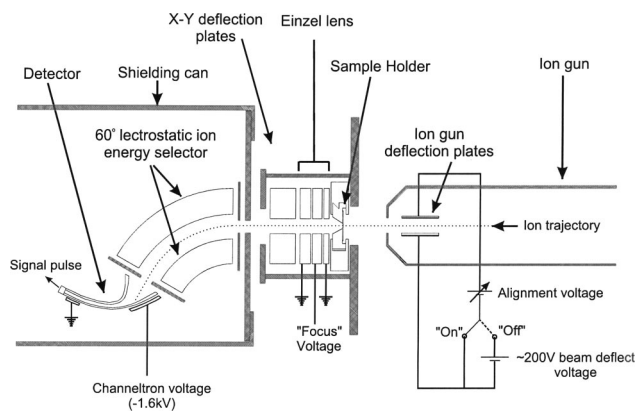


FIG. 3. Schematic of the ion optics. The manipulation of ions from the ion gun, through the sample membrane, and to the detector of the ion sculpting apparatus is illustrated.

ing membrane in the middle of the sample where the hole is located. The convergence angle of the beam is $\sim 7^\circ$. The ion flux is selected by adjusting the emission current of the ionizing electron filament. The argon gas pressure in the differentially pumped ion gun is typically maintained at 2×10^{-6} mbar by a leak valve.

The sample holder and the electrostatic optics responsible for refocusing the transmitted ions onto the detector are mounted behind a stainless steel plate hung from the “top” flange of the ion sculpting chamber. Pictures of the assembled flange, plate, and optics appear in Fig. 4. The steel plate provides both mechanical stability to the optics and shields the ion detector from stray ions coming from the ion gun. The electrostatic Einzel lens is located directly behind

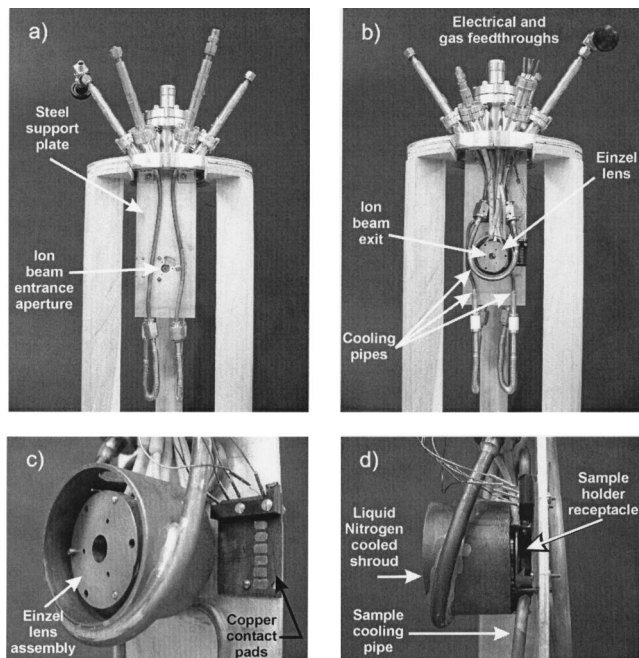


FIG. 4. The Einzel lens and sample receptacle assembly. The ion beam is incident on the sample from the front (a) through an aperture in the steel support plate. The Einzel lens, which is surrounded by a liquid nitrogen copper cooling shroud, focuses the beam which exits from the back (b). Detailed pictures show the copper contact pads (c) that provide electrical access to the sample holder, which slides into the dove-tail wedge shown in (d).

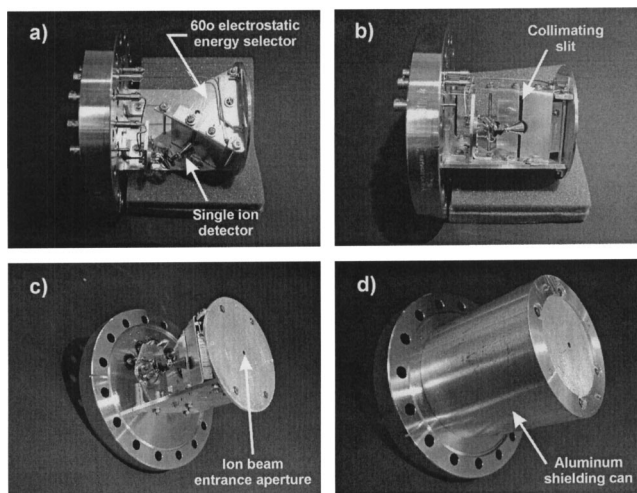


FIG. 5. The ion detection system and 60° electrostatic energy selection element. (a) Top view of the naked detection system. (b) Side view of the naked detection system. (c) Angle view of the naked flange. (d) Angle view of the shielded can.

the sample. The lens elements consist of three co-axial rings separated and electrically isolated from one another by sets of three precision ruby spacer balls (Edmund Industrial Optics, Barrington, NJ) squeezed between them. A typical “focus” voltage of 2.2 kV is applied to the central focusing lens element. The fringing fields that extend into the central region of the lens act to focus the ion beam. Two pairs of electrostatic deflection elements located behind the Einzel lens and oriented perpendicular to each other steer the ion beam horizontally and vertically to help direct it into the detector cup.

The ion detector and the 60° electrostatic deflection system are mounted on a stainless steel plate fixed to a flange at the “back” of the chamber. A picture of the mounted detector and deflection system appears in Fig. 5. The electrostatic deflection of the ion beam through 60° selects only 3 keV ions for detection, filtering out undesired counts arising from x rays produced in the ion gun or lower energy, stray ions arriving at the detector. The deflection system consists of two 60° concentric cylindrical sectors that have 1 cm spacing between them, and a 10 cm radius of curvature for the concentric central ion trajectory. A balanced 250 V potential difference applied between the plates induces an electric field that bends 3 keV ions to the detector, located at the output of the deflection plates. Grounded collimating slits at the front and back apertures of the deflection system ensure that stray electric fields do not deflect or defocus the ion beam entering or exiting the deflection system.

Some modification of a Burle electronics 4860 ion detector was necessary to fit it into the vacuum chamber. The cup of the detector is typically charged to -1.6 kV for ion detection, with the back of the detector held at ground. The detector efficiency (the fraction of ions that are counted) is expected to be 80% under our particular experimental conditions.

The deflection and detection system is further shielded from potential noise sources by encasing it in an aluminum can that contains only a single hole at the front through which the ion beam enters. A picture of the fully shielded

system is shown in Fig. 5(d). When the detector is completely obscured to the ion beam by a sample containing no apertures, the measured noise count rate does not exceed the expected Channeltron “dark noise” level of 1 count every ~ 20 s.

In order to align the ion beam with the sample and the detector, deflection and focus voltages are adjusted so as to maximize the transmitted ion count rate through a sample containing a hole. This process was originally aided by inserting a sample containing a ~ 50 μm aperture in the middle and by replacing the single ion detector with a multichannel plate (MCP) detector that could image the transmitted ion beam spot. The beam was first centered on the sample by adjusting the gun deflector and focus voltages to maximize the ion transmission through the aperture. The Einzel lens and post-sample deflection voltages were then adjusted to form a focused and centered spot on the MCP before replacing it with the single ion detector. The alignment of the ion optics was typically verified at the beginning of each ion sculpting experiment involving a sample with a prefabricated hole.

IV. VACUUM CONDITIONS

Since ion beam sculpting relies on the interaction of ion beams with a material surface, high vacuum conditions are needed to keep surfaces free of contaminants during an experiment, and to minimize the scattering of ions off gas molecules. A load-lock sample entry system that is vented with dry nitrogen minimizes exposure of the chamber to contaminants. A liquid-nitrogen-cooled copper shroud that condenses contaminants and improves the local vacuum near the sample surrounds both the sample holder and the optics as seen in Fig. 4. A Dycor 200M (Dycor Technologies, Edmonton, Canada) residual gas analyzer indicates that the principal component of the 1×10^{-9} mbar background pressure is water. Under these conditions, the maximum contamination rate (assuming that every molecule that impinges on a surface sticks to it) is one monolayer every 30 min, and the mean free path for molecules in the background gas is ~ 10 km.⁷

V. SAMPLE MANIPULATION

The ion sculpting feedback technique requires that structures to be modified with nanometer precision be fabricated in freestanding membranes. Standard microfabrication techniques were used to produce freestanding membranes of silicon-rich, low-stress silicon nitride (SiN), stoichiometric silicon nitride (Si₃N₄) and silicon dioxide (SiO₂) on silicon substrate. Other materials such as aluminum, chromium, polyimide, and polymethylmethacrylate have also been tested by depositing thin films on top of freestanding SIN membranes. Initial holes or bowl-shaped cavities were milled into the freestanding membranes using a focused ion beam (FIB) machine (FEI/Micrion 9500, FEI/Micrion, Peabody, MA).

Samples are mounted on the sample holder (Fig. 6), with the free-standing membrane aligned to the center of the holder with ~ 50 μm precision using an optical microscope. The ion beam typically impinges on the flat, “front” surface

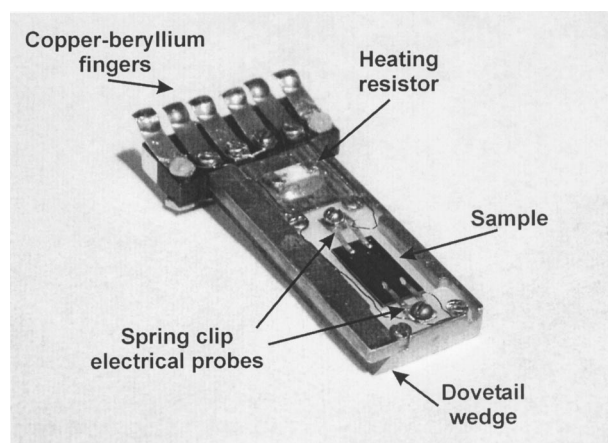


FIG. 6. Sample holder for the ion sculpting apparatus.

of samples whose FIB milling preparation was performed on the opposite side. A dovetail wedge on the sample holder guides it into its receptacle located in the chamber optics shown in Fig. 4(c), where it is kinematically locked into position by a spring clip. The temperature of a sample is monitored by a resistive temperature device (RTD) imbedded in the sample holder, and can be controlled with 1 °C precision using a 1 W, 50 Ω heating resistor glued to the top of the sample holder, and a gas-operated copper cooling pipe attached to the sample holder receptacle. The electric properties of devices such as tunneling electrodes fabricated on the surface of samples can be monitored via metallic spring clips. The RTD, the heating resistor, and the electrical probe clips connect to copper-beryllium fingers at the back of the sample holder, which slide into position above copper contact pads on the steel support plate, and allow all devices on the sample holder to be electrically accessed by electrical feedthroughs on the “top” flange.

VI. SYSTEM CONTROL AND AUTOMATION

The ion sculpting system is controlled by a computer via LABVIEW software. The principal function of the program is to monitor and record the count rate of ions transmitted through the nanopore, and terminate the ion sculpting process as soon as the desired hole size is obtained. The ion count rate is sampled for a fixed time interval (typically once per second) and the total counts recorded in that interval are compared to a selectable threshold. When the count rate crosses the threshold, the beam is automatically deflected off the sample using the electrostatic deflection plates at the ion gun output, halting the ion sculpting process. Since holes can be made to open or close, the program can trigger on the rising or falling slope of the count rate data.

A second important function of the automation software is to control the time structure of periodically pulsed ion beams applied to the sample. The use of ion beam pulses was first implemented to improve the resolution of nanopore fabrication because by shortening the duration of each ion beam pulse, the ion-induced change in hole size per pulse is decreased. This makes automated adjustment of the ion gun parameters such as ion flux unnecessary. It has been discovered that the duty cycle of a periodically pulsed ion beam has

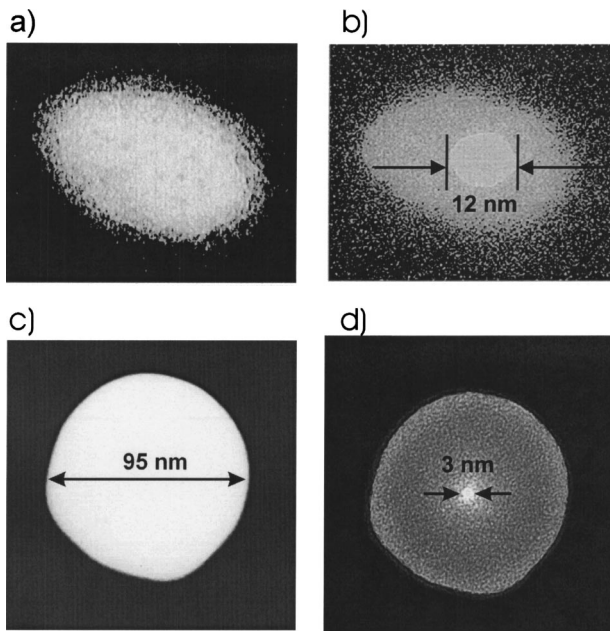


FIG. 7. Ion beam sculpting small holes in SiN. An initial bowl-shaped cavity (a) in a freestanding SiN film is opened to a 12 nm hole (b) by ion sculpting at -120°C . At room temperature (20°C), an initial 95 nm hole (c) is controllably closed to result in a 3 nm nanopore (d).

an important nonlinear effect on the dynamics of material transport under ion beam irradiation, which affords the ion sculpting apparatus greater control over the process.⁸ The duty cycle of a pulsed beam is defined by the times it spends “on” and “off” a sample (T_{on} and T_{off} , respectively). The start of each cycle is triggered by the Labview program. The duration of T_{on} is accurately determined by an external transistor–transistor logic one-shot (Global Specialties 4001 Pulse Generator, Global Specialties, Cheshire, CT). The difference between the sampling frequency and T_{on} determines T_{off} .

VII. NANOPORE FABRICATION AND MATERIAL TRANSPORT STUDY EXPERIMENTAL PROTOCOL

Prior to ion beam sculpting, the initial hole in each sample is inspected by transmission electron microscopy to provide a precise measure of its size. The measured area of the hole is used to calibrate the count rate of the ion sculpting apparatus: the ion flux is taken to be the initial count rate divided by the initial area of the hole. This procedure recalibrates the flux for each measurement to guarantee an accurate measure of the size of the hole by the transmitted ion current.

The sample is loaded from atmosphere into the main chamber within about ten minutes through the loadlock, which is evacuated in two stages. First a liquid-nitrogen-cooled sorption pump evacuates the loadlock to a pressure of $\sim 10^{-2}$ mbar. Then a turbomolecular pump evacuates the chamber to 10^{-6} mbar, at which point the sample can be loaded into the chamber through the load lock gate valve. The sample is typically given five minutes to equilibrate at its prescribed experimental temperature prior to ion beam sculpting.

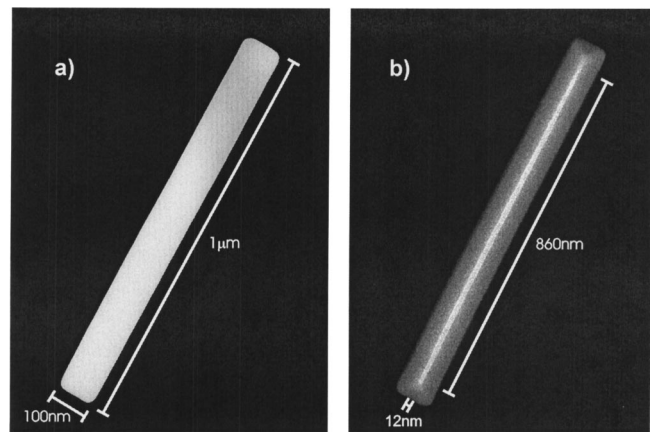


FIG. 8. Ion beam sculpting a nanoslit. A micron-long, 100 nm-wide slit in a SiN membrane (a) was ion sculpted to result in (b) a 12 nm-wide nanoslit.

An experiment or fabrication begins when the ion beam is first directed onto the sample. When an experiment or fabrication is completed the ion beam is deflected off the sample. For the fabrication of holes less than 5 nm in diameter, a final few short (≤ 100 ms) ion beam pulses are manually applied using the pulse generator to avoid early termination of the process by a premature low ion count.

VIII. PERFORMANCE

The use of feedback is the key to the function of the ion beam sculpting apparatus. The ability to register single transmitted ions provides real-time information on the size of a developing hole at the nanometer scale. This exquisite sensitivity makes the instrument particularly well-suited to the study of ion-stimulated matter transport, and enabled the discovery and characterization of a remarkable lateral matter transport process.^{3,8} At low temperatures and high incident ion flux, sputter erosion dominates at the hole boundary, resulting in the widening of the hole. Ion sculpting at high temperature, low ion flux, and long T_{off} for periodically pulsed beams stimulates the transport of material into the hole, resulting in the growth of a thin solid-state film from the hole boundary that controllably closes the hole. The physical understanding of ion beam sculpting that resulted from these studies had an important impact on our ability to craft nanopores through control over experimental parameters, and offered the distinct nanofabrication strategies of adding or removing matter with nanometer control.

Figure 7 illustrates two methods for fabricating nanopores by ion beam sculpting with a 3 keV argon ion beam. First, a bowl-shaped cavity in a freestanding SiN held at -120°C was exposed to a $2.6 \text{ Ar}^+ \text{ nm}^{-2} \text{ s}^{-1}$ beam incident on its flat side, and then halted when a 12 nm hole had been opened. In the second method, an initial 95 nm hole in a freestanding SiN membrane at 20°C was exposed to a $47 \text{ Ar}^+ \text{ nm}^{-2} \text{ s}^{-1}$ beam that resulted in the shrinking of the hole, which was controllably halted when the diameter of the hole reached 3 nm. For the routine fabrication of solid-state nanopores we prefer the latter technique because the progress can be continuously monitored by the stream of ions transmitted through the hole.

The closing of holes in a variety of materials by ion beam sculpting has been explored. By testing small holes in

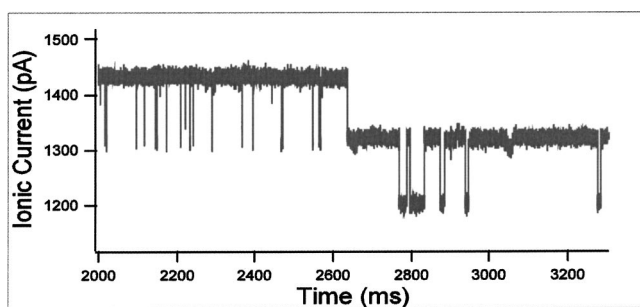


FIG. 9. An ion-sculpted nanopore serves as an electronic detector that is sensitive to individual DNA molecules. A 6 nm-wide SiN nanopore separated two reservoirs of 1 M KCl solution, across which 120 mV were applied. Individual DNA molecules in the negatively charged reservoir are detected as quantized diminutions of the ionic current through the nanopore.

thin films (~ 100 nm) that were supported on freestanding SiN membranes, we are able to close nanopores in films of aluminum, chromium, poly-methyl-methacrylate, and polyimide (Kapton). The ion beam sculpting apparatus has been unable to close holes in thin films of silver or gold with parameters so far explored.

In addition to fabricating nanopores, the ion sculpting apparatus is capable of tailoring the size of structures of different geometries with nanometer precision. Figure 8 shows an initial $100\text{ nm} \times 1\text{ }\mu\text{m}$ slit in SiN that was closed to form a $890\text{ nm} \times 12\text{ nm}$ “nanoslit” by ion beam sculpting at $58\text{ }^\circ\text{C}$, with a $\sim 2\text{ Ar}^+\text{ nm}^{-2}\text{ s}^{-1}$ pulsed beam whose duty cycle was $T_{\text{on}} = 100\text{ ms}$, $T_{\text{off}} = 900\text{ ms}$. We have fabricated nanoslits $20\text{ }\mu\text{m}$ long, and have observed nothing to suggest that this length has an upper limit. Extended nanoslits can be used as stencil masks for the deposition of nanowires.⁹

The ultimate confirmation of the utility of ion beam sculpting, for our initial purposes, lies in the fabrication of solid state nanopores for single molecule biophysics experiments. Figure 9 illustrates the success of this enterprise. The figure shows electronic signatures of individual DNA mol-

ecules translocating an ion-sculpted SiN nanopore detector in saline solution. In this experiment a 6 nm nanopore bridged two reservoirs of 1 M KCl ionic solution between which a 120 mV potential difference was applied. The introduction of 3-kilobase long ($\sim 1\text{ }\mu\text{m}$), double-stranded DNA to the negatively charged reservoir resulted in electrical pulses whose magnitude is clearly quantized. The current blockades are caused by the presence of a single molecule in the hole, restricting the ionic current through it by an amount proportional to the cross-sectional size of that molecule.³ The observed quantization is explained by the fact that only integer numbers of DNA strands can be present in the nanopore. Thus, the nanopore has been used to study molecular conformations during translocation.¹⁰

ACKNOWLEDGMENTS

The authors would like to acknowledge the assistance of Bob Quinlan, who helped machine and assemble much of the apparatus, as well as support from DARPA, DOE, NSF, and Agilent Technologies.

¹P. Y. Apel, Y. E. Korchev, Z. Siwy, R. Spohr, and M. Yoshida, *Nucl. Instrum. Methods Phys. Res. B* **184**, 337 (2001).

²K. S. Ralls, R. A. Buhrman, and R. C. Tiberio, *Appl. Phys. Lett.* **55**, 2459 (1989).

³J. Li, D. Stein, C. McMullan, D. Branton, M. J. Aziz, and J. A. Golovchenko, *Nature (London)* **412**, 166 (2001).

⁴A. Adams and F. H. Read, *J. Phys. E* **5**, 156 (1972).

⁵E. Harting and F. H. Read, *Electrostatic Lenses* (Elsevier, New York, 1976).

⁶J. H. Moore, C. C. Davis, and M. A. Coplan, *Building Scientific Apparatus: A Practical Guide to Design and Construction*, 2nd ed. (Perseus, Cambridge, MA, 1991).

⁷J. F. O'Hanlon, *A User's Guide to Vacuum Technology*, 2nd ed. (Wiley, New York, 1989).

⁸D. Stein, J. Li, and J. A. Golovchenko, *Phys. Rev. Lett.* **89**, 276106 (2002).

⁹M. M. Deshmukh, D. C. Ralph, M. Thomas, and J. Silcox, *Appl. Phys. Lett.* **75**, 1631 (1999).

¹⁰J. Li, M. Gershow, D. Stein, E. Brandin, and J. A. Golovchenko, *Nat. Mater.* **2**, 611 (2003).